ELSEVIER

Physica C 304 (1998) 225–238

PHYSICA C

Variational Monte Carlo study on the superconductivity in the two-dimensional Hubbard model

Kunihiko Yamaji [a,b,*], Takaashi Yanagisawa [a], Takeshi Nakanishi [a,1], Soh Koike [a,b]

[a] *Electrotechnical Laboratory, 1-1-4 Umezono, Tsukuba, Ibaraki, 305-8568, Japan*
[b] *Institute of Materials Science, University of Tsukuba, Ten-nodai, Tsukuba, 305-8573, Japan*

Received 29 May 1998; accepted 11 June 1998

Abstract

The possibility of superconductivity (SC) in the ground state of the two-dimensional (2D) Hubbard model was investigated by means of the variational Monte Carlo method. The energy gain of the *d*-wave SC state, obtained as the difference of the minimum energy with a finite gap and that with zero gap, was examined with respect to dependences on U, electron density ρ and next nearest neighbor transfer t' mainly on the 10×10 lattice. It was found to be maximized around $U = 8$ (the energy unit is nearest neighbor transfer t). It was shown to sharply increase for negative values of t' and have a broad peak for $t' \sim -0.10$. For these value of t' the energy gain was a smooth increasing function of ρ almost independent of the shell structure in the region starting from ~ 0.76 up to the upper bound of investigation 0.92. This clearly indicates that the result is already close to the value in the bulk limit. For $t' = 0$, the energy gain depended on the electronic shell state. This suggests the 10×10 lattice is not sufficiently large for this case, although it is highly plausible that the bulk limit value is finite. Competition between the SC and the commensurate SDW states was also investigated. When $t' = 0$, the ground state is SDW in the range of $\rho \geq \sim 0.84$. The SC region slightly extends up to ~ 0.87 for $t' \sim -0.10$. Consequently the present results strongly support an assertion that the 2D Hubbard model with $t' \sim -0.1$ drives SC by itself in the ρ region from ~ 0.76 to ~ 0.87. The above features are in a fair agreement with the phase diagram of the optimally and overly hole-doped cuprates. The energy gain in the SC state with suitable parameters is found to be in reasonable agreement with the condensation energy in the SC state of $YBa_2Cu_3O_7$. The corresponding t–J model proves to give an order-of-magnitude larger energy gain, which questions its validity.

PACS: 74.20.Mn; 74.25.Bt; 74.25.Dw; 74.72.− h

Keywords: Two-dimensional Hubbard model; Variational Monte Carlo method; *d*-wave superconductivity; SDW; Next nearest neighbor transfer; Condensation energy

1. Introduction

Recently the mechanisms of superconductivity (SC) in high-temperature cuprate superconductors and organic superconductors have been extensively

* Corresponding author. Electrotechnical Laboratory, 1-1-4 Umezono, Tsukuba, Ibaraki 305-8568, Japan. Tel.: +81-298-54-5368; Fax: +81-298-54-5099; E-mail: yamaji@etl.go.jp

[1] Present address: Institute of Physical and Chemical Research, 2-1 Hirosawa, Wako 351-0198, Japan.

0921-4534/98/$ - see front matter
PII: S0921-4534(98)00283-4

studied using various two-dimensional (2D) models of electronic interactions. The 2D Hubbard model is the simplest and the most fundamental one among such models. Early studies of this model using the quantum Monte Carlo (M.C.) method indicated the existence of an attractive interaction for SC [1]. However, this possibility has been controversial. Some authors asserted from quantum M.C. results that the enhanced SC correlation does not develop into the predominant one at low temperatures or in the ground state of this model [2–5]. Some authors supported this possibility by numerical results using the variational M.C. method [6]. Since it is of prime importance to establish the simplest electronic model for superconductivity and since these early studies had shortcomings due to the restrictions to the investigated parameter space, the problem deserves more extensive investigation from various aspects such as dependences on the system size, the on-site Coulomb energy U, the electron density ρ and the next nearest neighbor transfer energy t'. Recently, appropriate values of t' were found to remarkably enhance SC correlations [7–9]. We apply the variational M.C. method [10,11] mainly to the 10×10-site system with electron numbers from 68 to 92. This method has a merit that it allows to treat larger values of U than the quantum M.C. methods. We revisit the issue investigated in Ref. [6], carrying out more extensive study with higher precision in a wider parameter space. In a previous preliminary report [12] we worked out a variational Monte Carlo calculation with 84 electrons on the 10×10 lattice and confirmed that the 2D Hubbard model has the d-wave SC state. In the present work, first, we examine the U-dependence of the energy gain due to the condensation into the SC state and find the optimal value of U is about 8 in units of the nearest neighbor transfer energy t. In the previous report we confirmed that the energy gain in the SC state sharply increases with the introduction of t' with a negative value. In this report we calculate the energy gain as a function of t' in a sufficiently wide range for a fixed value of $U = 8$ and show that it has a broad peak around a negative value $t' \sim -0.1$. The approximate peak energy gain in the SC state, i.e., at $t' \sim -0.1$, is plotted as a function of electron density ρ together with that for $t' = 0$. When $t' \sim -0.1$, the energy gain starts to be finite at about $\rho = 0.68$ and increases fairly smoothly with increase of ρ in the range of $0.76 \leq \rho \leq 0.92$. We carried out calculations in both cases of open and closed shells. The smoothness of the energy gain against ρ indicates that the dependence of the energy gain on the shell structure is weak, in contrast to the case with $t' = 0$, and that the results are already close to the bulk limit. This means that the 2D Hubbard model with $t' \sim -0.1$ has a definite bulk-limit energy gain per site in the SC state. While when $t' = 0$, the energy gain in the closed shell state was found much smaller than that in the open shell state. This indicates that the 10×10 lattice is not sufficiently large for the case of $t' = 0$, contrary to the case of $t' \sim -0.1$, although a kind of average of the results in both shell states is very probable to give a finite energy gain per site in the bulk limit. Of course it is needed to treat larger lattices with $t' = 0$ but some important findings at the present stage are considered to deserve a report, with the latter problem left to be settled, since with larger sizes computation needs extremely long time.

Thirdly, we calculate the energy gain in another ordered state, i.e., spin density wave (SDW) state. We treat the SDW with a fixed wave vector (π, π). Here the length unit is the lattice constant. The energy gain in the SDW state was found to quickly drop with decrease of ρ from unity and to vanish at ρ just below 0.84 when $t' = 0$. However, at $\rho = 0.84$ the SDW state was slightly more stable than the SC state so that the boundary between both states lies just below $\rho = 0.84$ for $t' = 0$. t' is known to destabilize the SDW in the hole-doped state, while it promotes SC pairing. We study to what extent the phase boundary between the competing SC and SDW states is affected by the negative t'. The boundary is appreciably pushed up to the higher ρ side with increase of the absolute value of the negative t', although not largely.

We point out that the resultant SC region from $\rho \sim 0.76$ to $\rho \sim 0.86$ and the increased SC energy gain with increase of ρ are in accord with experimental features of cuprate high-T_c superconductors in the overdoped region. The observed energy gain in the SC state is found to be in fair agreement with the experimental condensation energy estimated from the critical magnetic field H_c and the specific heat of $YBa_2Cu_3O_7$. On the other hand the t–J model as an

effective Hamiltonian of the Hubbard model is noticed to give an enormous overestimation of the condensation energy.

In Section 2 the model and the method are described. Results on the SC and SDW ground states are given in Sections 3 and 4, respectively. In Section 5, the obtained results are compared with experiments and also with other computational works. Section 6 gives the summary. Short reports on the present results were given in Refs. [12,13].

2. Model and method

Our model is the 2D Hubbard model defined by

$$H = -t \sum_{\langle ji \rangle, \sigma} \left(c^{\dagger}_{j\sigma} c_{l\sigma} + H_{\mathrm{c}} \right) + U \sum_{j} c^{\dagger}_{j\uparrow} c_{j\uparrow} c^{\dagger}_{j\downarrow} c_{j\downarrow}, \tag{1}$$

where $c^{\dagger}_{j\sigma}$ ($c_{j\sigma}$) is the creation (annihilation) operator of an electron with spin σ at the jth site; the sites form a rectangular lattice; t is the transfer energy between the nearest-neighbor (n.n.) sites; t is our energy unit; $\langle jl \rangle$ denotes summation over all the n.n. bonds. U is the on-site Coulomb energy. In this report, we also study the effect of t' between n.n.n. sites by including

$$H_{\mathrm{nnn}} = -t' \sum_{\langle\langle jl \rangle\rangle, \sigma} \left(c^{\dagger}_{j\sigma} c_{l\sigma} + H_{\mathrm{c}} \right) \tag{2}$$

in the Hamiltonian; in the above equation $\langle\langle jl \rangle\rangle$ means summation over the n.n.n. pairs.

Our trial wave function is a Gutzwiller-projected BCS-type wave function defined as [10,11]:

$$\Psi_{\mathrm{s}} = P_{N_{\mathrm{e}}} P_{\mathrm{G}} \psi_{\mathrm{BCS}}, \tag{3}$$

$$\psi_{\mathrm{BCS}} = \prod_{\boldsymbol{k}} \left(u_{\boldsymbol{k}} + v_{\boldsymbol{k}} c^{\dagger}_{\boldsymbol{k}\uparrow} c^{\dagger}_{-\boldsymbol{k}\downarrow} \right) |0>, \tag{4}$$

where P_{G} is the Gutzwiller projection operator given by

$$P_{\mathrm{G}} = \prod_{j} \left[1 - (1-g) n_{j\uparrow} n_{j\downarrow} \right]; \tag{5}$$

g is a variational parameter in the range from 0 to unity and j labels a site in the real space. $P_{N_{\mathrm{e}}}$ is a projection operator which extracts only the states with a fixed total electron number N_{e}. Coefficients $u_{\boldsymbol{k}}$ and $v_{\boldsymbol{k}}$ appear in our calculation only in the ratio defined by

$$v_{\boldsymbol{k}}/u_{\boldsymbol{k}} = \Delta_{\boldsymbol{k}} \Big/ \left(\xi_{\boldsymbol{k}} + \sqrt{\xi^2_{\boldsymbol{k}} + \Delta^2_{\boldsymbol{k}}} \right), \tag{6}$$

$$\xi_{\boldsymbol{k}} = -2t\left(\cos k_x + \cos k_y\right) - 4t' \cos k_x \cos k_y - \mu, \tag{7}$$

where $\Delta_{\boldsymbol{k}}$ is a $\boldsymbol{k}$-dependent gap function defined later; μ is a variational parameter working like the chemical potential in the trial wave function; $c_{k\sigma}$ is the Fourier transform of $c_{j\sigma}$. Neglecting constant factors, Ψ_{s} can be rewritten as

$$\Psi_{\mathrm{s}} \sim P_{N_{\mathrm{e}}} P_{\mathrm{G}} \exp\left[\sum_{\boldsymbol{k}} \left(v_{\boldsymbol{k}} + u_{\boldsymbol{k}} \right) c^{\dagger}_{\boldsymbol{k}\uparrow} c^{\dagger}_{-\boldsymbol{k}\downarrow} \right] |0>, \tag{8}$$

$$\Psi_{\mathrm{s}} = P_{N_{\mathrm{e}}} P_{\mathrm{G}} \exp\left[\sum_{j,l} a(j,l) c^{\dagger}_{j\uparrow} c^{\dagger}_{l\downarrow} \right] |0>, \tag{9}$$

$$\Psi_{\mathrm{s}} \sim P_{\mathrm{G}} \left[\sum_{j,l} a(j,l) c^{\dagger}_{j\uparrow} c^{\dagger}_{l\downarrow} \right]^{N_{\mathrm{e}}/2} |0>, \tag{10}$$

$$\Psi_{\mathrm{s}} = P_{\mathrm{G}} \sum_{j_1, \ldots, j_{N_{\mathrm{e}}/2}, l_1, \ldots, l_{N_{\mathrm{e}}/2}} A\left(j_1, \ldots, j_{N_{\mathrm{e}}/2}, l_1, \ldots, l_{N_{\mathrm{e}}/2}\right) \times c^{\dagger}_{j_1\uparrow} c^{\dagger}_{j_2\uparrow}, \ldots, c^{\dagger}_{j_{N_{\mathrm{e}}/2}\uparrow} c^{\dagger}_{l_1\downarrow} c^{\dagger}_{l_2\downarrow} \ldots, c^{\dagger}_{l_{N_{\mathrm{e}}/2}\downarrow} |0>, \tag{11}$$

where $a(j,l)$ is defined by

$$a(j,l) = (1/N_{\mathrm{s}}) \sum_{\boldsymbol{k}} \left(v_{\boldsymbol{k}}/u_{\boldsymbol{k}} \right) \exp\left[i\boldsymbol{k} \cdot \left(R_l - R_j \right) \right], \tag{12}$$

with N_{s} being the number of sites and

$$A(j_1, j_2, \ldots, j_{N_{\mathrm{e}}/2}, l_1, l_2, \ldots, l_{N_{\mathrm{e}}/2}) = \begin{vmatrix} a(j_1,l_1) & a(j_1,l_2) & \ldots & a(j_1,l_{N_{\mathrm{e}}/2}) \\ a(j_2,l_1) & a(j_2,l_2) & \ldots & a(j_2,l_{N_{\mathrm{e}}/2}) \\ \vdots & \vdots & & \vdots \\ a(j_{N_{\mathrm{e}}/2},l_1) & a(j_{N_{\mathrm{e}}/2},l_2) & \ldots & a(j_{N_{\mathrm{e}}/2},l_{N_{\mathrm{e}}/2}) \end{vmatrix}; \tag{13}$$

$j_1, j_2, \ldots$ are arranged in the ascending order; so are l_1, l_2, ... Then the ground state energy

$$E_{\mathrm{g}} = \langle H \rangle \equiv \langle \Psi_{\mathrm{s}} | H | \Psi_{\mathrm{s}} \rangle / \langle \Psi_{\mathrm{s}} | \Psi_{\mathrm{s}} \rangle \tag{14}$$

is obtained using a M.C. procedure [10,11]. In order to minimize computation time in the M.C. computation the values of the cofactors of the matrix in Eq. (13) were stored and corrected at each time when the electron distribution was modified. Errors accumulated in the cofactors after corrected were avoided many times by recalculating cofactors as determinants, instead of getting them by correction, after a certain number of M.C. steps. We tested our programs using exact diagonalization results for small systems. We optimized E_g with respect to g, $\Delta_{\boldsymbol{k}}$ and μ. In the later stage of work we employed the correlated measurements method [14,15] in the process of searching optimal parameter values minimizing E_g. It enables to precisely locate the minimum position.

3. Results for the superconducting ground state

3.1. Case of the simple 2D Hubbard model

We studied the cases of the *d*-, extended *s*-(s^*-) and *s*-wave gap functions as follows:

$$\begin{aligned} d \quad & \Delta_{\boldsymbol{k}} = \Delta(\cos k_x - \cos k_y), \\ s^* \quad & \Delta_{\boldsymbol{k}} = \Delta(\cos k_x - \cos k_y), \\ s \quad & \Delta_{\boldsymbol{k}} = \Delta. \end{aligned} \tag{15}$$

The sizes of the lattice we treated are 6×6 and 10×10 having electron density close to unity with slight hole doping into the half-filled state.

Results indicating the occurrence of the *d*-wave superconductivity were obtained even for the case of $N_e = 32$ on the 6×6 lattice with the periodic and the antiperiodic boundary conditions (b.c.'s) for the *x*- and the *y*-direction, respectively, with $U = 8$ and $t' = 0$. This set of b.c.'s was chosen so that $\Delta_{\boldsymbol{k}}$ does not vanish for any $\boldsymbol{k}$-points possibly occupied by electrons; otherwise zero division occurs in Eq. (12). E_g/N_s is minimized at $\Delta \sim 0.10$. Here $g = 0.3038$ and $\mu = -0.48$. The energy gain due to the SC gap formation, i.e., SC condensation energy, was estimated at ~ 0.00028/site from the difference between the minimum and the intercept of the E_g-vs.-Δ curve with the vertical axis.

Main results written in this report were obtained for the 10×10 lattice with the same boundary conditions. Calculated energies per site for several types of wave functions with $N_e = 84$ on the 10×10 lattice are shown in Fig. 1 for the case of $U = 8$ and $t' = 0$. Here E_g/N_s is plotted as a function of Δ for the three types of gap functions given in Eq. (15). With the lattice, the b.c.'s and $N_e = 84$, the electronic shell structure in the limit of $U = 0$ is open, i.e., some $\boldsymbol{k}$-points are partially filled, as is illustrated in Fig. 2, which displays the electron occupancy at the $\boldsymbol{k}$-points. At each value of Δ in Fig. 1, $g = 0.30$ was chosen as the initial value of g and then the optimal value of μ was found by the least squares fit of E_g as a function of μ to a parabola. Using this value of μ, g was optimized again. Since E_g was a smooth function of g, the obtained optimal g and μ are sufficiently accurate. Using these parameter values, E_g was obtained as the average of the results of eight M.C. calculations each with 5×10^7 steps at $\Delta = 0.01$, 0.04 and 0.08 for the *d*-wave. The standard deviations were less than 0.00011. At other points, the numbers of M.C. calculations and steps were different but their error bars were within 0.00015 with the total M.C. steps greater than 2×10^8. The diamond shows the normal state value, -0.73585 ± 0.00024, obtained from 20 M.C.

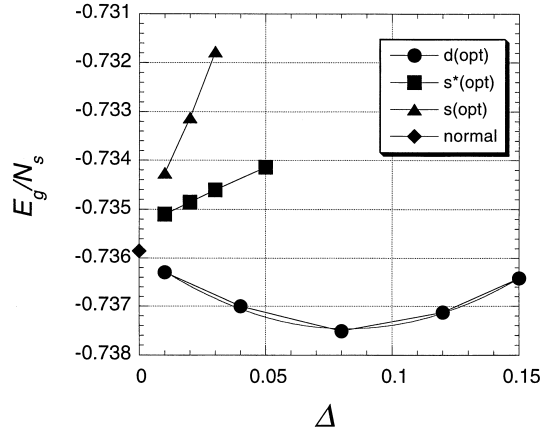

Fig. 1. Computed ground state energy per site E_g/N_s is plotted against Δ for the case of 84 electrons on the 10×10 lattice with $U = 8$ and $t' = 0$. Filled circles are for the *d*-wave gap function with g and μ optimized for each Δ. Filled squares and triangles are for the s^*- and *s*-wave gap functions, respectively. The diamond shows the normal state value. Straight lines between data points are the guide for the eye. The thin curve is a parabola given by the mean-squares fit to the *d*-wave data.

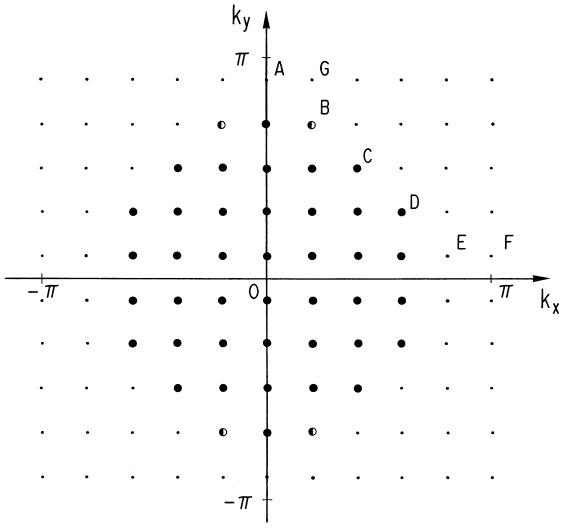

Fig. 2. Distribution of k-points in the reciprocal lattice in the case of the 10×10 lattice with the boundary conditions mentioned in the text. Closed and empty circles denote doubly occupied and empty sites, respectively, and circles partially closed are partially occupied sites in the case of 84 electrons. A, B, …, G label k-points lying in the neighborhood of the Fermi energy for later use.

calculations each with 10^7 steps, using the Gutzwiller-projected normal state wave function. In the employed normal state $(\pi/5,\ 7\pi/10)$ and $(-\pi/5,-7\pi/10)$ are fully occupied but $(\pi/5,\ -7\pi/10)$ and $(-\pi/5,7\pi/10)$ are unoccupied in the component of the trial wave function prior to the Gutzwiller projection.

Clearly, E_g/N_s is minimum at a finite value of $\Delta\approx0.08$ in the case of the d-wave gap parameter. The optimal parameter values at $\Delta=0.08$ are $g=0.3037$ and $\mu=-0.4263$. The least squares fit of a parabola to E_g/N_s as a function of Δ is of good quality, as seen in Fig. 1 and gives the minimum at $\Delta\cong0.082$. The curves of E_g/N_s for the s- and s^*-wave gap functions have definite positive slopes at small Δ and are extrapolated for $\Delta=0$ to ~-0.7354 and ~-0.7353, respectively, which are practically equal. These values are slightly higher than the value ~-0.73605 given by extrapolating the d-wave fitting parabola to $\Delta=0$. The normal state value of $E_g/N_s=-0.73585$ lies between the two groups of extrapolated values. The differences are due to a kind of size effect, as was explained in the previous report [12]. These differences in the case of 10×10 lattice are much smaller than the depth of the minimum of the d-wave curve.

The energy gain per site in the d-wave state was obtained from the parabola fitting to the energy-vs.-Δ curve as its depth of the minimum in reference with the intersection of the fitting curve with the vertical axis as $\sim0.00155/\text{site}$. It is five times larger than that for $N_e=32$ and $N_s=36$. This suggests that the size effect is considerable in the 6×6 system. This energy gain per site in the case of $N_s=100$ and $N_e=84$ is of the order of magnitude of the BCS superconducting condensation energy $\sim(\text{state density})\times\Delta^2\approx0.0010$ since the state density per site per spin around this density is approximately equal to $1/2\pi$ in units of t.

In order to check the superconducting nature of the ground state with a finite value of Δ, the correlation functions of BCS pair operators were calculated. Superconducting pair correlation functions $D_{\alpha\beta}(l)$, $\alpha,\ \beta=x,\ y$, are defined as:

$$D_{\alpha\beta}(l)=\langle\Delta_\alpha^\dagger(i+l,j)\,\Delta_\beta(i,j)\rangle, \tag{16}$$

where $\Delta_\alpha(i,j)$, $\alpha=x,\ y$, denote the annihilation operators of singlet electron pairs staying on n.n. sites as:

$$\Delta_x(i,j)=c_{ij\downarrow}\,c_{i+1,j\uparrow}-c_{ij\uparrow}\,c_{i+1,j\downarrow}, \tag{17}$$

$$\Delta_y(i,j)=c_{ij\downarrow}\,c_{i,j+1\uparrow}-c_{ij\uparrow}\,c_{i,j+1\downarrow}, \tag{18}$$

where $c_{ij\sigma}$ means the annihilation operator at site (i,j) with spin σ. The average $\langle\ldots\rangle$ is defined in Eq.

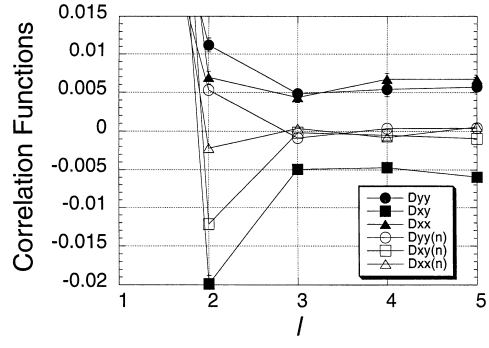

Fig. 3. Parts of the correlation functions $D_{\alpha\beta}$ of superconducting pair operators for case of the d-wave minimum state shown in Fig. 1. The horizontal axis is the distance l between two positions of two pair operators. Closed symbols are for the superconducting state and open ones for the normal state. $D_{\alpha\beta}$ is defined by Eq. (16).

(14). The result for a state close to the minimum E_g point in Fig. 1, i.e., $\Delta = 0.078$, $\mu = -0.428$ and $g = 0.30$, is shown in Fig. 3. The vertical scale is enlarged to highlight the long range parts. The correlation extends over the whole lattice as expected, showing a clear contrast to the normal state. The *d*-wave nature appears in the negative sign of $D_{xy}(l)$ for $l = 2$–5.

3.2. U-dependence

The *U*-dependence of the energy gain in the SC state is shown in Fig. 4 with the same values of N_s and N_e. The energy gain was determined from the depth of the minimum, as explained above. Except for the above-mentioned case of $U = 8$, the minimum position defined by optimal Δ, g and μ was determined by means of the correlated measurements and E_g was calculated for this position with the same number of M.C. steps as for $U = 8$. Next, E_g for $\Delta = 0.01$ was obtained and then the fitting parabola allowed us to get the energy gain. The energy gain in this definition gives the condensation energy in the SC state in the present approximation. The energy gain has the maximum for about $U = 8$. It quickly decreases with decrease of *U*. It gradually decrease with increase of *U* over 12. In contrast, the value of optimal Δ is nearly proportional to *U* up to $U = 12$ and then saturates for larger *U*.

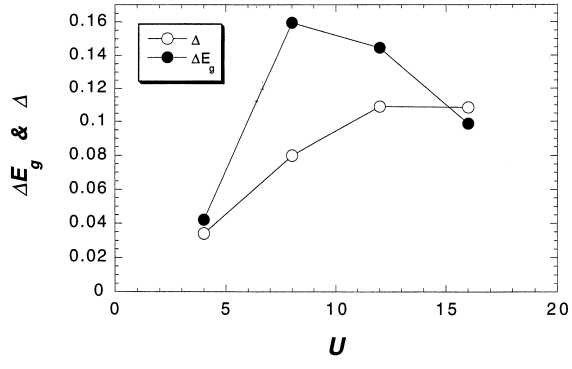

Fig. 4. Energy gain ΔE_g (closed circles) and gap parameter Δ (open circles) in the superconducting state are plotted against on-site Coulomb energy *U* for the same system as in Fig. 1.

3.3. t′-Dependence

In the 2D Hubbard and the 2D *d*–*p* models, the one-electron state density increases peak-wise around the energy of the van Hove singularities located in the *k*-space region around $(0, \pi)$ and $(\pi, 0)$. When t' is negative in the 2D Hubbard model with H_{nnn} the energy level of van Hove singularity moves toward the Fermi energy in the hole-doped systems, as is seen from Eq. (7), which realizes a situation favorable to get superconductivity for most theories. In fact Shimahara and Takada showed that in the RPA framework T_c increases with the introduction of t' [16]. Importance of t' in the physics of high-T_c cuprates was pointed out in Ref. [17]. From the viewpoint of the two-band mechanism of superconductivity in which the pair-wise transfer of electrons from a certain $\boldsymbol{k}$-region to another $\boldsymbol{k}$-region promotes SC, the location of the $\boldsymbol{k}$-space region highly contributing to the state density in the neighborhood of the Fermi energy should lead to a larger energy gain in the SC state [18,19a,19b]. The state density peak is known to be further enhanced with the increase of electron correlation, as the single-particle dispersion along the lines from these points to (0, 0) becomes anomalously weak [20]. The increased state density around the singularity has been argued to enhance T_c of the *d*-wave superconductivity [21]. The value of t' was argued to correlate with the maximum T_c values of cuprate subfamilies [7,8]. Quantum M.C. studies indicated that t' enables the bulk superconductivity in the 2D Hubbard model [9].

We have examined the t'-dependence of the energy gain, taking account of H_{nnn} in Eq. (2) in our model. In the case of $N_e = 32$ on the 6×6 lattice, the energy minimum became slightly deeper with the change of t' from zero to -0.25, but at $t' = 0.25$ the minimum became shallower by a factor of 2. In the case of $N_e = 84$ on the 10×10 lattice the energy gain was maximized around $t' \cong -0.1$ to -0.15 as shown in Fig. 5. The error bar for $\Delta E_g/N_s$ in the figure is about 0.0003. Δ is also displayed in the figure with the right-hand-side vertical scale. The error bar for Δ is about 10% of the magnitude. With a positive value of $t' = 0.10$, the energy gain quickly decreases, nearly vanishing when $t' = 0.25$. It also nearly vanishes for $t' \sim -0.40$. Fig. 6 shows the SC pair correlation functions as functions of the distance

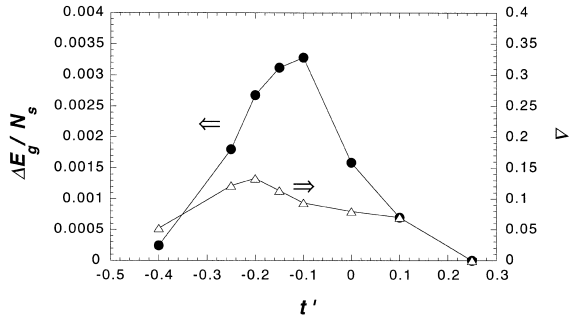

Fig. 5. Energy gain per site $\Delta E_g / N_s$ in the superconducting state is plotted by closed circles with the left vertical scale as a function of next nearest neighbor transfer energy t' in the case of 84 electrons on the 10×10 lattice with $U=8$. Values of Δ are shown by open triangles with the right-hand-side vertical scale.

between pair operators in the optimal state for the case of $t'=-0.10$. At the farthest distance their values are twice larger that those for $t'=0$ (Fig. 3), as expected. Thus, an appropriate negative value of t' enhances the *d*-wave SC in the hole-doped case in the Hubbard model, which is in qualitative agreement with the above-mentioned references. The t'-dependences of the energy gain and Δ in the case of $N_e=80$ exhibited in Fig. 7 show similar features as in Fig. 5.

When one plots one-electron levels (Fig. 8), $\varepsilon_k = \xi_k + \mu$, for $\boldsymbol{k}$-points in the non-interacting limit as a function of t', a few occupied levels and a few empty levels are found to be bunched into a close neighborhood of the Fermi energy ε_F within ±0.07 as t' takes -0.1 to -0.15. These levels are located

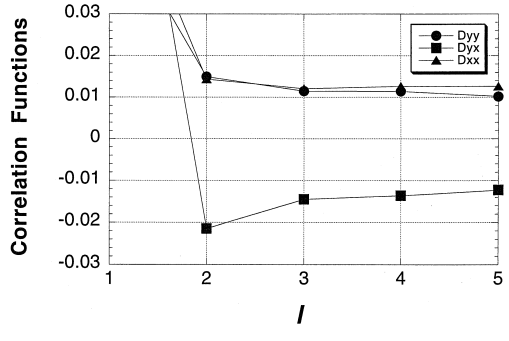

Fig. 6. Parts of the correlation functions of superconducting pair operators for the case of the largest SC energy gain in Fig. 5 with $t'=-0.10$, $\Delta=0.0941$, $g=0.3003$, and $\mu=-0.6152$. The notation is the same as in Fig. 3.

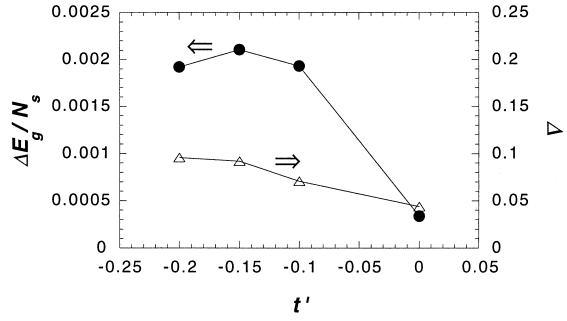

Fig. 7. ΔE_g and Δ as functions of t' in the case of $\rho=0.80$. Other parameter values are the same as in Fig. 5.

in the $\boldsymbol{k}$-space mainly in the neighborhood of the level of the van Hove singularity. Since each one-electron level is orbitally four- (or rarely two-) fold degenerate due to symmetry, the number of one-electron states whose levels are located in the neighborhood of ε_F is considerable. Since such a feature is known to enhance the SC pair correlation functions in the two-chain Hubbard model [19a,19b] even in strongly correlated situations, this feature is considered to bring about the remarkable increase of the energy gain. Although the particular peaking location of t' may be slightly size-dependent since the one-electron levels are size-dependent, such a concentration of one-electron levels around ε_F is considered to occur for any system size when the appropriate negative t' pushes down the van Hove singularity

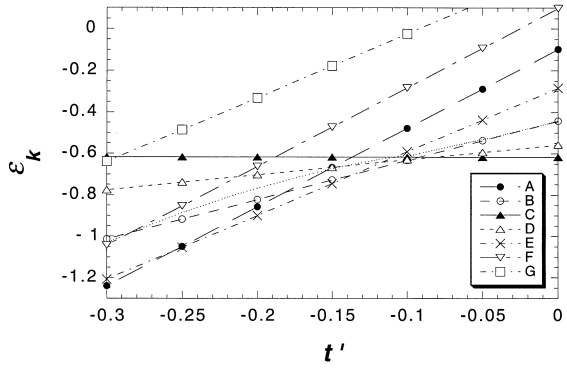

Fig. 8. One-electron levels ε_k of k-points A, B, …, G in the neighborhood of ε_F are plotted as functions of t'. Due to orbital and spin degeneracies, each levels can accommodate eight electrons except the A level which can accept four. The dotted curve exhibits ε_F in the case of the $U=0$ limit.

close to ε_F. Therefore, this effect should work even in the bulk limit.

3.4. Electron-density dependence

Fig. 9 shows the energy gain per site in the SC state as a function of the electron density $\rho = N_e/N_s$ for the cases of $t' = 0$, -0.10 and -0.15. The corresponding values of Δ as a function of ρ are exhibited in Fig. 10. When $t' = -0.10$ whose curve is exhibited with closed circles, the cases of $\rho = 0.68$, 0.76, 0.84 and 0.92 have an open shell, in another word, there are partially filled $\boldsymbol{k}$-points in the electronic state in the $U = 0$ limit, as is shown in Fig. 2 for $N_s = 10 \times 10$ and $N_e = 84$ with $t' = 0$. While the other cases with $\rho = 0.72$, 0.80 and 0.88 have a closed shell. The curve has almost no dependence on the shell state in the region of $0.76 \le \rho \le 0.92$, making a definite contrast with the case with $t' = 0$ described later. This suggests that the curve is already close to the bulk limit one in this region. For $t' = -0.15$ with open diamonds, the cases of $\rho =$ 0.68, 0.76 and 0.88 have an open shell while others have a closed shell. Here we observe a weak dependence on the shell structure. However the deviation from the rough average between the open-shell and closed-shell curves are only of the order of $1/10$ of the average energy gain per site in the region of $0.76 \le \rho \le 0.92$, which is small enough to judge that the points are already close to the bulk limit. The smooth dependence on ρ is also observed in the SC gap amplitude Δ for $t' = -0.10$ and -0.15 in Fig. 10. These results clearly support a statement that the 2D Hubbard model with $t' \sim -0.1$ gives a finite condensation energy for the *d*-wave SC state in the bulk limit in the region of ρ from ~ 0.76 to ~ 0.86. For $\rho = 0.72$ a minimum with finite Δ was obtained in both cases of $t' \sim -0.1$. But the SC energy gain was within the error bound so that $\Delta E_g/N_s \sim 0$. For $\rho = 0.68$ a finite value was obtained for both cases but it is so small that it may not remain finite in the bulk limit.

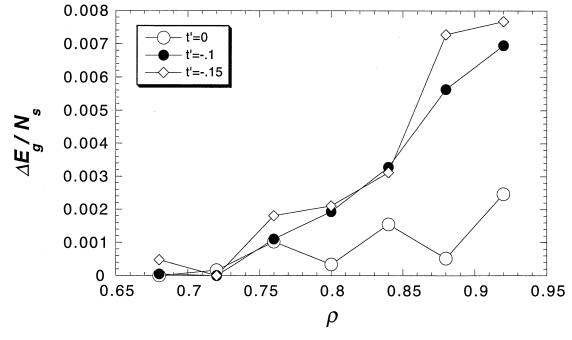

Fig. 9. Energy gain per site $\Delta E_g / N_s$ in the superconducting state against electron density ρ. Open circles are for $t' = 0$, closed ones for $t' = -0.1$ and closed diamonds for $t' = -0.15$. The lattice is 10×10 and $U = 8$.

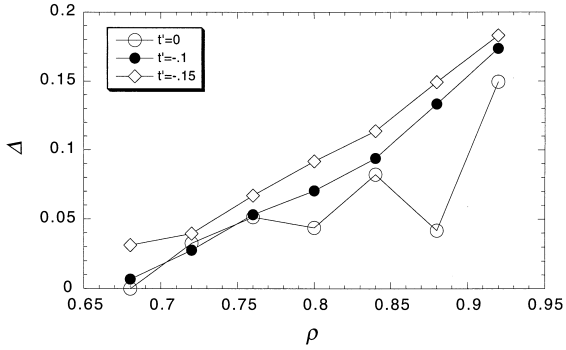

Fig. 10. Amplitude of the gap function Δ is plotted as functions of ρ for $t' = 0$, -0.10 and -0.15, corresponding to the $\Delta E_g / N_s$ vs. ρ curves in the preceding figure. The error bar is about 0.01 for $\rho \sim 0.92$. For $\rho \sim 0.7$ it is about 0.005.

Open circles for $t' = 0$ in Fig. 9 form a zigzag curve as a function of ρ. Relatively larger are the energy gains for $\rho = 0.76$, 0.84 and 0.92, for which the electron shell is open. The values for the cases of $\rho = 0.72$, 0.80 and 0.88 with closed shell are smaller. This shell dependence is a system-size effect and indicates that the 10×10 lattice is not sufficiently large when $t' = 0$. It suggests also that the larger the SC energy gain is, the smaller the sufficient system size is. However, the average curve between the two curves formed of the points of both kinds of shell states is expected to be a highly probable approximation to the bulk limit and the model with $t' = 0$ is also probable to drive SC, although more extensive calculation with large lattices is needed to remove the room for doubt. Incidentally, for $\rho = 0.68$, no finite energy gain was obtained although the shell is open.

In Fig. 1 of the precursive work of Giamarchi and Lhuillier [6] we find a corresponding value for the

SC energy gain per site. It is for $\rho = 0.8125$ on the 8×8 lattice with $U = 10$ and $t' = 0$. Our value for $\rho = 0.80$ on the 10×10 lattice with $U = 8$ and $t' = 0$ should be close to the value. The shell structure for $\rho = 0.8125$, or $N_e = 52$, on the 8×8 lattice is closed; so is the case with $\rho = 0.80$ on the 10×10 lattice. However, our value is 3.38×10^{-4}, being about $1/3$ of the above-mentioned value, and if we put it in their figure it is located in the lower end part of the large error bar attached to the data point. In the above-mentioned figure the energy gain vanishes around $\rho \sim 0.56$ but in Fig. 9 of the present work it vanishes around $\rho \sim 0.72$. We believe that the present results are more improved than the results of Giamarchi et al. because of improved accuracy of computation.

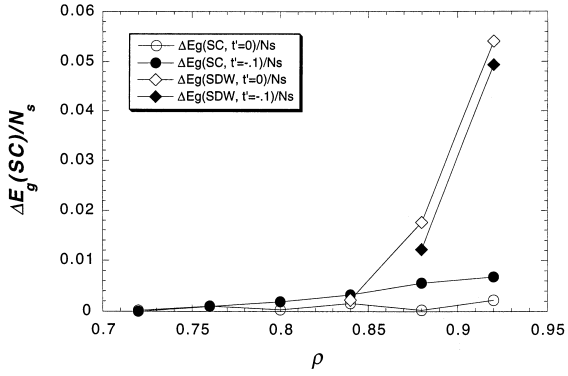

Fig. 11. Energy gain per site $\Delta E_g / N_s$ in the SDW state against electron density ρ is plotted for $t' = 0$ (open diamond) and for $t' = -0.10$ (closed diamond). Error bar is about 0.0003. $\Delta E_g / N_s$ in the superconducting state is also plotted again with the same symbols as in Fig. 9 with the diminished vertical scale.

4. Competition with the SDW state

4.1. Magnetic state of the 2D Hubbard model

When the density of doped holes is small or zero, the 2D Hubbard model takes an antiferromagnetic state as its ground state. With increase of doped hole density, the magnetic order is destroyed and SC appears. At what hole density does the SC state start? We have investigated the transition between the pure SC and the pure uniform SDW states by computing the energy of the SDW state by means of the variational Monte Carlo method. The trial SDW wave function is written as [22,11]

$$\Psi_{\mathrm{SDW}} = P_{\mathrm{G}} \psi_{\mathrm{SDW}}, \tag{19}$$

$$\psi_{\mathrm{SDW}} = \prod_{\boldsymbol{k}} \left(u_{\boldsymbol{k}} c^{\dagger}_{\boldsymbol{k}\uparrow} + v_{\boldsymbol{k}} c^{\dagger}_{\boldsymbol{k}+Q\uparrow} \right) \times \prod_{\boldsymbol{k}'} \left(u_{\boldsymbol{k}'} c^{\dagger}_{\boldsymbol{k}'\downarrow} - v_{\boldsymbol{k}'} c^{\dagger}_{\boldsymbol{k}'+Q\downarrow} \right) |0>, \tag{20}$$

$$u_{\boldsymbol{k}} = \left[\left(1 - w_{\boldsymbol{k}} / \sqrt{w_{\boldsymbol{k}}^2 + M^2} \right) / 2 \right]^{1/2}, \tag{21}$$

$$v_{\boldsymbol{k}} = \left[\left(1 + w_{\boldsymbol{k}} / \sqrt{w_{\boldsymbol{k}}^2 + M^2} \right) / 2 \right]^{1/2}, \tag{22}$$

$$w_{\boldsymbol{k}} = (\varepsilon_{\boldsymbol{k}} - \varepsilon_{\boldsymbol{k}+Q}) / 2, \tag{23}$$

$$\varepsilon_{\boldsymbol{k}} = \xi_{\boldsymbol{k}} + \mu, \tag{24}$$

where P_{G} is the Gutzwiller projection operator defined by Eq. (5). Summation over $\boldsymbol{k}$ and $\boldsymbol{k}'$ in Eq. (20) is performed over the filled $\boldsymbol{k}$-points, as in the calculation of the normal state variational M.C. energy. Q is the SDW wave vector equal to (π, π). M is the SDW potential amplitude.

4.2. Phase boundary between SC and SDW states

As shown by the open diamonds in Fig. 11, the energy gain per site in the SDW state rises very sharply from $\rho \sim 0.84$ in the case of $t' = 0$. Already at $\rho = 0.84$ it takes 0.0023 and is slightly larger than that in the SC state. However, at $\rho = 0.80$ there is no more stable SDW state. By extrapolating the sharply

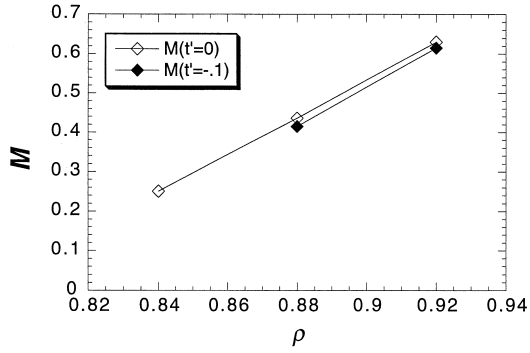

Fig. 12. Optimized value of SDW gap parameter M is plotted as a function of ρ for two values of $t' = 0$ (open diamond) and -0.10 (closed diamond), corresponding to two SDW curves in Fig. 11.

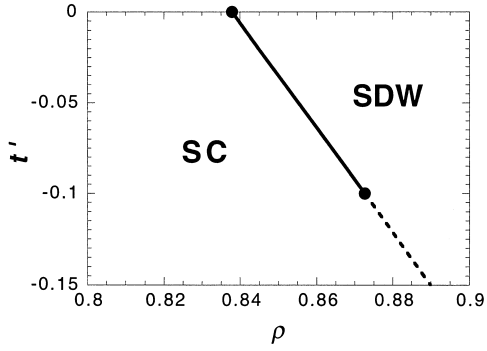

Fig. 13. Phase diagram of superconducting (SC) and SDW phases in cuprates high-T_c superconductors in the plane of temperature T vs. electron and hole densities. The thick curve was decided as written in the text. The dotted line is an extrapolation.

rising curve of the SDW energy gain per site as a function of ρ, the boundary between the SDW and the SC states is given at $\rho = 0.838$. Optimized values of M are plotted in Fig. 12.

Since finite t' deteriorates the nesting property of the Fermi surface, the energy gain per site in the SDW state should decrease with introduction of negative t'. The calculated values for $t' = -0.10$ is shown in Fig. 11 by closed diamonds. The energy gain per site in the SC state given by closed circles increases when $t' = -0.10$. The phase boundary between the two is estimated at about 0.873 as the intersection of the extrapolation of the line linking the two closed diamonds and the curve for the SC energy gain per site with $t' = -0.10$. So the boundary is pushed up by $\Delta\rho = 0.035$ but not enough as to move the boundary up to $\rho = 0.95$, the observed boundary in $La_{2-x}Sr_xCuO_4$ [23]. The obtained phase diagram in the $t' - \rho$ plane is shown in Fig. 13.

5. Comparison with experiments and other results

5.1. Energy gain per site in the SC state

By means of the cell-perturbation method, Feiner et al. [24] were able to reduce the d–p model into an effective one-band Hubbard model. In their result the transfer energy t slightly depends on the occupancy on the two related sites. Using typical parameter values for the d–p model t is estimated at 0.51 eV for hole transfer. U is estimated at 3.4 eV so that $U/t = 6.7$. With this relatively small U the authors derive an appropriate value of exchange interaction constant J for the t–J model, appearing later, thanks to the ferromagnetic interaction term and the Coulomb interaction between nearest neighbor sites in the effective one-band Hubbard model. These values of t and U are common for the cuprate high-T_c superconductors. The t' value was estimated at around -0.06 eV, i.e., -0.12 in units of t, for hole-type superconductors. They observed that its weak dependence on each cuprate is correlated with the values of T_c among the cuprates. Since the additional spin-dependent ferromagnetic term and nearest neighbor Coulomb interactions are relatively small, the 2D Hubbard model without these additional interaction but with the above-mentioned parameter values should give a right magnitude of the SC energy gain if it actually gives a finite value.

For $U = 8$ and $t' = 0$ the maximum SC energy gain per site is approximately given by the value at $\rho = 0.84$ in the neighborhood of the SC-SDW phase boundary. It is about 0.0010 as the average of the values for both shell states. For $U \approx 6.7$ this value should diminish by a factor $3/4$ according to Fig. 4 so that the calculated maximum SC energy gain per site is 0.00038 eV/site, if we take $t = 0.51$ eV. The value of t' for hole conduction was evaluated by several authors at, e.g., -0.06 eV [25,24], -0.124 eV (for the La system) [26], and -0.17 eV [27] for hole-doped cuprates. If we take $t' = -0.06$ eV $\cong$ -0.12 given by Feiner et al. [24], the above energy gain should be multiplied by a factor 2.0 and becomes 0.00076 eV/site. Incidentally, this value of t' is in the range of the optimal energy gain, $t' \cong -0.1$ to -0.15.

According to Hao et al. [28] the critical magnetic field $H_c(0)$ at zero temperature was estimated to be 1.10 T for $YBa_2Cu_3O_7$. From the expression $H_c^2/8\pi$ for the condensation energy in the SC state, the experimental value for the SC energy gain per site is equal to 0.00026 eV per Cu site in layers. Triscone et al. [29] gave slightly larger values of H_c for two samples of $YBa_2Cu_3O_7$, 1.231 and 1.364 T, corresponding to condensation energies 0.00033 and 0.00040 eV/(Cu site), respectively.

Another source of information on the condensation energy is the specific heat reported by Loram et

al. [30] on $YBa_2Cu_3O_7$. By numerically integrating the SC specific heat minus the normal-state one with respect to temperature from zero to just T_c, the condensation energy was obtained as 0.000168 eV/(Cu site). Since the appreciable fluctuation contribution is observed at temperatures above T_c, which is recognized as the maximum position of the specific heat, and since it was simply neglected, this value is in fair agreement with the value given from the critical field.

The above-mentioned calculated value of the maximum SC energy gain per site is in reasonable agreement with the experimental SC condensation energy in view of simplifications and uncertainties in the parameter values of the model. This agreement strongly indicates that the 2D Hubbard model includes essential ingredients for the SC in the cuprate superconductors.

The present results of the energy gain per site in the SC state can be compared with the results for the t–J model. For the value of exchange interaction constant $J = 4t^2/U = 0.5$ corresponding to $U = 8$, Fig. 7 in Ref. [31] by Yokoyama and Ogata allows to estimate the SC energy gain per site calculated for the t–J model. At $\rho = 0.84$ it is $0.026t$. This is 17 times larger than that obtained for the 2D Hubbard model at the same electron density in Section 3. If we take 0.0010 for the SC energy gain per site of the 2D Hubbard model, judging from the average of the open and closed-shell curves, the ratio is 26. Since the 2D Hubbard model has been found to give a sound SC condensation energy as seen above, we have to judge that the fault is on the 2D t–J model as an effective Hamiltonian of the 2D Hubbard model, i.e., it gives too large an SC condensation energy at least in the parameter region where $J/t \sim 1/2$. This means that the t–J model made of the leading two terms in the expansion in powers of t/U of the canonical transformation of the Hubbard model should be treated together with the higher-order terms for it to give a realistic SC condensation energy.

The t–J model is derived also starting from the d–p model or three-band Hubbard model. As such its parameter values are derived in literatures. The values are given in wide ranges, even by a single group. The value of t is estimated at 0.224 eV by Tohyama and Maekawa [26] for the La system, at 0.51 eV by Feiner et al. [24], in the range of 0.29–0.98 eV by Batista and Aligia [32]. The value of J is obtained at 0.13 eV for La_2CuO_4 from Raman scattering data [33]. Theoretical values given by these authors for typical cases are around this value. If we take $J = 0.13$ eV and $t = 2J$, the SC energy gain of the 2D t–J model with $\rho = 0.84$ is estimated at $0.026t = 0.0068$ eV/site by using the model in Ref. [31]; it is 26 times larger than the value obtained from Hao et al.'s H_c value. Around this value of $J/t = 0.5$ the SC energy gain of the t–J model is considered to be roughly proportional to $t \cdot J/t = J$, if the SC energy gain of the model with normalized coupling constant J/t is roughly proportional to J/t. Then, the above-mentioned large ratio applies to the most parameter sets. Only when J/t becomes so small, e.g., with increase of t, that SC almost vanishes, the above ratio may decrease to unity. Thus with plausible parameter sets, the t–J model is very probable to give too large a SC condensation energy. Again the higher order correction terms must not be neglected, for the model to work properly at least concerning the SC condensation energy, so that they oppose to the occurrence to SC [32]; the present result does not support the correction terms of the type that facilitate SC [34].

5.2. Phase diagram in the T_c-*vs.*-ρ plane

According to our results in Section 4, in the case of small negative t' the SC region extends from $\rho \sim 0.76$ to $\rho \sim 0.86$ with smoothly increasing SC condensation energy with increase of ρ. This suggests that in this ρ region T_c is finite and smoothly increases with increase of ρ. The range of this ρ region and the expected smooth increase of T_c are in fair agreement with the features of the T_c-vs.-p ($p = 1 - \rho$, doped-hole density) phase diagram in the optimal to overdoped region, i.e., $0.15 \leq p \leq 0.25$ or $0.75 \leq \rho \leq 0.85$, where T_c increases with increasing ρ [23].

Corresponding to the underdoped region with $0.05 \leq p \leq 0.15$, the present results do not give an SC region but give an SDW region. However, there is a possibility that more elaborate calculations give a kind of SC phase where SC and SDW coexist and that the phase diagram in the underdoped region is also provided by the 2D Hubbard model. The reasons are as follows: Giamarchi and Lhuillier [6]

showed that a uniform wave function describing the coexistence of SC and SDW gives a lower energy than the pure SDW wave function in the system of 32 electrons on the 6×6 lattice. We have checked on the 10×10 lattice that such a coexistence wave function is possible only in the ρ region higher than the above-mentioned boundary between SC and SDW. Therefore, in the higher ρ region there may be a coexistence phase in a certain region. However, there are no experiments confirming a uniform coexistence except for recent reports suggesting a non-uniform coexistence in $La_{1.6-x}Nd_{0.4}Sr_xCuO_4$ [35]. Further, stripe-type solutions are known to give a lower total energy for the SDW state in the low hole-doping region [36]. Therefore, the above-mentioned uniform coexistence state may be dominated by a more complicated non-uniform way of coexistence of SC and SDW. Such a ground state could be obtained only if we use sufficiently large sizes of the system, as is the case with the SDW stripe solutions [36]. With this speculated coexistent SC state, we expect that T_c is maximum at the above-mentioned phase boundary at $\rho \sim 0.86$, since the plausible coexistence state should have T_c lower than the value of T_c at the boundary due to a smaller electron density carrying SC properties. At temperatures higher than T_c, the SDW ordering without the SC one may remain. Such a coexistent SC state may be consistent with the feature of the T_c–p phase diagram in the underdoped region [23]. Of course, all these possibilities remain to be confirmed with actual calculations.

5.3. Comments on the quantum Monte Carlo results

Whether the 2D Hubbard model drives SC or not has been an important unsettled issue for theoretical and computational physics. Although quantum M.C. studies recognized the enhancement of the SC susceptibility, dominance of SC has not been confirmed. However, the numerical studies have been under severe restrictions to the parameter values in which reliable results were obtainable, e.g., with respect to the system size, value of U/t, temperature and so on. Within these few years the occurrence of the SC was strongly indicated when t' is introduced [8,9,37]. When the shell structure approaches to the open one, even if it was closed, SC correlations were observed to be much enhanced [38]. On the contrary, recently Zhang et al. showed that SC features weaken with increase of the system size with U up to $8t$ [39]. However, the state with $\rho = 0.85$ and $t' = 0$ with which their main results are exhibited is located in the SDW region according to our results. With this value of ρ the dominant SDW is considered to have diminished the SC correlations for some values of U. Even in the case where the coexistence of SC and SDW might have occurred, the SC features should have been different from what we expect in the usual uniform superconducting state. Therefore, their results do not disprove the existence of SC in the ρ region where we find SC dominating. Further, the quantum M.C. calculations were done for closed-shell electron densities. This shell state must have led to a very small energy gain and weakened the SC features when the system size is not sufficiently large. The distribution of the single particle energy $\varepsilon_{\boldsymbol{k}}$ around the Fermi energy are scarce in the cases they treated. These reasons are suspected to have made the SC features in their work very weak. A study with an elaborate method allowing high precision is under way searching enhanced SC correlations with appropriate values of ρ [40].

6. Summary

Using the variational Monte Carlo method we have investigated the dependencies of the energy gain per site in the SC state on important parameters such as on-site Coulomb energy U, next nearest neighbor transfer energy t' and electron density per site ρ. We worked mainly with the 10×10 lattice. The energy gain is maximized at about $U = 8$. It is maximized for $t' = -0.10$ to -0.15, reaching twice the value at $t' = 0$. This increase of the SC energy gain was ascribed to the fact that a high density of the one-electron levels around the van Hove singularity go close to ε_F due to an appropriate negative value of t'. The SC pair correlation functions increased correspondingly. With $U = 8$ and $t' = -0.10$ or -0.15, the energy gain starts to be finite at $\rho \sim 0.68$, smoothly increasing with increase of ρ from $\rho = 0.76$ up to $\rho = 0.92$ up to which we have made calculation. The curves of the energy gain as a

function of ρ have only a weak dependence on the shell structure or on whether some of the $\boldsymbol{k}$-points are partially filled or not (open or closed shell) in the $U = 0$ limit electron distribution. This definitely suggests that the curves are already close to the bulk limit ones. On the other hand, with $U = 8$ and $t' = 0$, the energy gain in the open shell state is sizable but that in the closed shell state is rather suppressed so that the obtained values seem to have still appreciable system size dependence, although the average curve between the open- and closed-shell curves is considered to be a fair approximation to the bulk limit. We have also calculated the energy gain in the commensurate SDW state. It sharply rises as a function of ρ starting at about $\rho \sim 0.84$ for $\rho = 0$, making the SDW state the lower energy state in the higher ρ region above this value. A finite value of $t' \sim -0.1$ brought about an upward shift of the boundary by $\Delta t' \sim 0.035$. Therefore, our calculations confirmed that the electronic repulsive interaction can drive SC by itself in the region from $\rho \sim 0.76$ up to the boundary at $\rho \sim 0.87$ with $t' \sim -0.1$. The maximum SC energy gain per site in the SC region was found to be close to the experimental SC condensation energy evaluated from H_c and the specific heat of $YBa_2Cu_3O_7$. On the other hand, the corresponding t–J model was pointed out to give a value enormously larger by a factor exceeding 20, indicating that it is not quantitatively reliable as a model for high-T_c cuprates without taking account of higher-order correction terms. The feature of the experimental phase diagram in the T_c–ρ plane in the region of ρ lower than the ρ of the maximum T_c was asserted to be in a good agreement with our results. These results strongly suggest that the simple 2D Hubbard model includes essential ingredients of high-T_c cuprates. A speculative argument on the higher ρ region outside our SC region was given concerning the coexistence of SC and SDW.

Acknowledgements

The authors are cordially thankful to Dr. T. Giamarchi, Professor J. Kondo, Dr. K. Kuroki, Professor T. Moriya, Professor M. Ogata and Dr. R. Ramakumar for valuable discussions.

References

[1] J.E. Hirsch, Phys. Rev. Lett. 54 (1985) 1317.
[2] S.R. White, D.J. Scalapino, R.L. Sugar, E.Y. Loh, J.E. Gubernatis, R.T. Scaletar, Phys. Rev. 40 (1989) 506.
[3] N. Furukawa, M. Imada, J. Phys. Soc. Jpn. 61 (1992) 3331.
[4] D. Scalapino, in: High Temperature Superconductivity—the Los Alamos Symposium—1989 Proceedings, K.S. Bedell, D. Coffey, D.E. Deltzer, D. Pines and J.R. Schrieffer (Eds.), Addison-Wesley Publ. Comp., Redwood City, 1990, p. 314.
[5] E. Dagotto, Rev. Mod. Phys. 66 (1994) 763.
[6] T. Giamarchi, C. Lhuillier, Phys. Rev. B 43 (1991) 12943.
[7] R. Raimondi, J.H. Jefferson, L.F. Feiner, Phys. Rev. B 53 (1996) 8774.
[8] L.F. Feiner, J.H. Jefferson, R. Raimondi, Phys. Rev. Lett. 76 (1996) 4939.
[9] T. Husslein, I. Morgenstern, D.M. Newns, P.C. Pattnaik, J.M. Singer, H.G. Matuttis, Phys. Rev. B 54 (1996) 16179.
[10] H. Yokoyama, H. Shiba, J. Phys. Soc. Jpn. 56 (1987) 1490.
[11] C. Gros, Ann. Phys. (New York) 189 (1989) 53.
[12] T. Nakanishi, K. Yamaji, T. Yanagisawa, J. Phys. Soc. Jpn. 66 (1997) 294.
[13] K. Yamaji, T. Yanagisawa, T. Nakanishi, S. Koike, in Proc. 10th Int'l Symp. on Superconductivity (ISS'10), Oct. 1997, Gifu, Advances in Superconductivity X, I. Osamura and I. Hirabayashi (Eds.), Springer, Tokyo, 1998.
[14] C.J. Umriger, K.G. Wilson, J.W. Wilkins, Phys. Rev. Lett. 60 (1988) 1719.
[15] K. Kobayashi, K. Iguchi, Phys. Rev. B 47 (1993) 1775.
[16] H. Shimahara, S. Takada, J. Phys. Soc. Jpn. 57 (1988) 1044.
[17] T. Tanamoto, H. Kohno, H. Fukuyama, J. Phys. Soc. Jpn. 62 (1993) 717.
[18] J. Kondo, Prog. Theor. Phys. 29 (1963) 1.
[19a] K. Yamaji, Y. Shimoi, Physica C 222 (1994) 349.
[19b] K. Yamaji, Y. Shimoi, T. Yanagisawa, Physica C 235–240 (1994) 2221.
[20] Z.-X. Shen, W.E. Spicer, D.M. King, D.S. Dessau, B.O. Wells, Science 267 (1995) 343.
[21] A. Nazarenko, E. Dagotto, Phys. Rev. B 53 (1996) R2987.
[22] H. Yokoyama, H. Shiba, J. Phys. Soc. Jpn. 56 (1987) 3582.
[23] H. Takagi, T. Ido, S. Ishibashi, M. Uota, S. Uchida, Y. Tokura, Phys. Rev. B 40 (1989) 2254.
[24] L.F. Feiner, J.H. Jefferson, R. Raimondi, Phys. Rev. B 53 (1996) 8751.
[25] M.S. Hybertson, E.B. Stechel, M. Schlüter, D.R. Jennison, Phys. Rev. 41 (1990) 11068.
[26] T. Tohyama, S. Maekawa, J. Phys. Soc. Jpn. 59 (1990) 1760.
[27] H. Eskes, G.A. Sawatzky, L.F. Feiner, Physica C 160 (1989) 424.
[28] Z. Hao, J.R. Clem, M.W. McElfresh, L. Civale, A.P. Malozemoff, F. Holtzberg, Phys. Rev. B 43 (1991) 2844.
[29] G. Triscone, B. Revaz, A.F. Khoder, J.-Y. Genoud, A. Junod, J. Muller, Physica C 235–240 (1994) 1557.
[30] J.W. Loram, K.A. Mirza, J.R. Cooper, W.Y. Liang, Phys. Rev. Lett. 71 (1993) 1740.

[31] H. Yokoyama, M. Ogata, J. Phys. Soc. Jpn. 65 (1996) 3615.
[32] C.D. Batista, A.A. Aligia, Phys. Rev. B 48 (1993) 4212.
[33] Y. Tokura, S. Koshihara, T. Arima, H. Takagi, S. Ishibashi, T. Ido, S. Uchida, Phys. Rev. B 41 (1990) 11657.
[34] H. Matsukawa, K. Okamoto, Czech. J. Phys. 46, suppl., pt. S5 (1996) 2647 [Proc. LT21].
[35] J.M. Tranquada, J.D. Axe, N. Ichikawa, A.R. Moodenbaugh, Y. Nakamura, S. Uchida, Phys. Rev. Lett. 78 (1997) 338.
[36] T. Giamarchi, C. Lhuillier, Phys. Rev. B 42 (1990) 10641.
[37] Y. Asai, Autumn Meeting of Phys. Soc. Jpn., 1996.
[38] K. Kuroki, H. Aoki, Phys. Rev. B 56 (1997) R14287.
[39] S. Zhang, J. Carlson, J.E. Gubernatis, Phys. Rev. Lett. 78 (1997) 4486.
[40] Y. Yanagisawa, S. Koike, K. Yamaji, Spring Meeting of Phys. Soc. Jpn., 1998.